Proceedings in Manufacturing Systems, Volume 20, Issue 1, 2025, pp. 35-41 ISSN 2067-9238

INTEGRATION OF CAD-GUIDED AUTOMATED INSERT PLACEMENT FOR ENHANCED 3D PRINTED COMPONENT ASSEMBLY

Dragoș-Alexandru CAZACU[1,*], Teodor-Cristian NAȘU[2], Mihail HANGA[3], Carmen-Cristiana CAZACU[4], Florina CHISCOP[4]

[1)] Eng., PhD, Education Team, PTC Eastern Europe SRL, Bucharest, Romania,
[2)] Student, Industrial Engineering and Robotics Fac, National University of Science and Technology POLITEHNICA Bucharest, Romania,
[3)] Master Student, Industrial Engineering and Robotics Fac., National University of Science and Technology POLITEHNICA Bucharest, Romania,
[4)] Lecturer, PhD, Robots and Manufacturing Systems Dep., National University of Science and Technology POLITEHNICA Bucharest, Romania

Abstract: *The paper presents an automated system for embedding brass threaded inserts into 3D-printed parts, reducing the variability of manual methods (misalignment, insufficient heating, excessive force) and the limitations of directly printed small threads (M4 and below). Target applications include rapid prototyping, low-volume production, and functional parts in aerospace and automotive sectors, where reliable joints enable repeated assembly. The device reads insert coordinates from Onshape (Parametric cloud CAD) via mate connectors (custom orientation systems in Onshape), ensuring faithful design-to-execution transfer. Its kinematics use a compact H-structure with a single-belt XY stage driven by stepper motors, plus a four-screw Z axis for uniform vertical motion and high stiffness. Inserts are automatically fed from a gravity tube through a servo-actuated lever and separator, then embedded with a heated tool head monitored by a thermocouple—tuned to 225 °C for PLA and 265 °C for ABS. A capacitive touch sensor provides real-time depth control (6 mm for M3, 8 mm for M4), while an inverted vise secures the workpiece above the tool head for optimal access. Integrating CAD data with Python motion-control scripts yields a low-operator workflow that improves repeatability and scalability. Tests on 3D printed parts of PLA and ABS with 3 to 6 perimeters show positional accuracy of ±0.05–0.07 mm, cycle times of 3.8–4.6 s per insert, and repeatability with 0.025–0.035 mm standard deviation—improving efficiency over manual methods by 73–75%. Thanks to modular design, compatibility with standard CAD platforms, and potential for adaptive tool heads, the system is well-suited for integration into automated additive-manufacturing post-processing lines and broader industrial adoption.*

Key words: *3D Printing, Threaded Inserts, CAD, Automation, Precision, Brass, Motion, Bonding.*

1. INTRODUCTION

Additive manufacturing (AM), commonly known as 3D printing, has revolutionized the production of complex geometries for functional applications, enabling rapid prototyping, low-volume manufacturing, and customized parts across industries such as aerospace, automotive, and medical device production. However, the integration of robust, repeatable threaded joints, a critical requirement for mechanical fastening and repeated assembly–disassembly cycles, remains a significant challenge. Directly printed threads, especially for small dimensions (≈ M4 and below), often suffer from weak interlayer bonding and dimensional inaccuracies due to limitations in printer resolution and material properties [1, 2]. These issues compromise structural integrity and render printed threads unreliable for demanding applications. As a result, brass threaded inserts have become a preferred solution, offering enhanced durability and joint strength. Yet, manual insertion of these inserts introduces variability through misalignment, inconsistent heating, or excessive force, leading to reduced part quality, unreliable connections, and inefficiencies in production workflows. One failed insert will scrap a full part that had taken many hours and material to print.

Prior efforts to address these challenges have predominantly relied on manual or semi-automated processes, with limited exploration of fully automated solutions. A notable CNC-based approach by Hanga et al. [3] demonstrated the feasibility of coupling CAD data with motion control for insert placement, leveraging precise kinematics inspired by 3D printing systems. However, such systems often lack seamless CAD-to-execution pipelines, closed-loop depth control, and efficient insert feeding mechanisms, leaving gaps in scalability and repeatability. Other studies [4] have explored printer-inspired designs, such as belt-driven motion systems and synchronized screw actuation, but their application to post-processing tasks like insert embedding remains underexplored.

This paper introduces a novel CAD-guided system for automated brass insert placement in 3D printed parts, designed to overcome the limitations of both direct thread printing and manual insertion. The system extracts insert coordinates directly from Onshape CAD models

* Corresponding author: Splaiul Independenței 319, 060044 Bucharest, Romania,
Tel.: +40 731 367 624;
E-mail addresses: *acazacu@ptc.com* (D.-A. Cazacu).

using mate connectors, ensuring precise translation from digital design to physical execution. It employs a compact H-structure with a single-belt XY stage driven by stepper motors for planar motion, complemented by a four-screw Z-axis drive for uniform vertical actuation, achieving high stiffness and positional accuracy. Inserts are fed from a gravity-based tube via a servo-actuated lever and separator, heated to material-specific temperatures. An inverted vise-like fixture secures the workpiece above the tool head, optimizing access and minimizing displacement. Integrated with Python-based motion control scripts, the system forms a streamlined, operator-minimal workflow from digital model to embedded insert.

The novelty of this work lies in its tight integration of CAD-derived coordinates with automated motion control, including coordinate extraction and base-relative transformations, combined with an innovative inverted fixturing strategy and closed-loop depth detection. These features enable precise, repeatable, and scalable insert placement, addressing critical gaps in prior work.

The authors' contributions include: (i) a modular mechatronic design optimized for insert embedding, balancing compactness and precision; (ii) a CAD-to-motion software tool chain for automatic coordinate retrieval, transformation, and sequencing, enhancing workflow automation; and (iii) a comprehensive evaluation protocol and dataset demonstrating significant gains in accuracy, speed, and repeatability. This system paves the way for scalable, reliable post-processing in additive manufacturing, with potential applications in automated assembly lines for functional parts.

2. PROBLEM DESCRIPTION

The 3D-printing industry has undergone major improvements in recent years — most notably in 3D printing precision, material diversity, and overall reliability. Despite this progress, the automated integration of threaded inserts remains largely unexplored [5]. Most current solutions still depend on manual heat-set processes that are sensitive to operator technique and introduce variability, which in turn reduces repeatability and part quality. Prior work by Hanga et al. demonstrated, in a CNC-based setup, that coupling CAD data with automated motion control is feasible for insert placement [3]. Building on these principles, the present work leverages design concepts common to 3D printers [3–4], such as belt-driven XY motion and synchronized screw actuation on Z, to develop a dedicated system for automatic placement of brass threaded inserts. This line of inquiry underscores how mature mechanisms from additive manufacturing can be adapted to address a post-processing problem that has received comparatively little research attention.

In functional AM applications, mechanical fastening and repeated assembly–disassembly cycles are routine, making reliable threaded connections critical. Directly printing threads is an appealing one-step option, but it faces well-documented limitations [1]. Fine thread geometries concentrate stresses and rely on narrow filaments of polymer, where insufficient interlayer bonding around small gaps can lead to weak root regions and premature failure. Additionally, many printers struggle to reproduce small threads (M4 and below) with adequate dimensional fidelity, especially when slicer line widths and layer heights approach or exceed feature size, yielding poor fit, rough flank surfaces, and, in practice, unusable connections [2]. These geometric and process constraints are exacerbated by polymer shrinkage, anisotropy, and staircase effects on inclined flanks, all of which degrade both strength and gauge conformity.

Brass heat-set inserts are widely adopted to overcome these issues, adding metal-to-metal engagement and locally reinforcing the joint. However, manual insertion introduces its own failure modes. Typical defects include tilt or angular misalignment caused by poor normal-to-surface control; too high temperature or too much time of heating, that will form a gap between the part and the insert; insufficient heating that prevents adequate wetting of insert knurls and produces weak bonding; and excessive force or over-dwell that collapses bosses, imprints tooling, or drives resin melt beyond the intended boundary. These errors are tightly coupled to an operator's real-time judgment of temperature, angle, and pressure, and they tend to worsen with operator fatigue.

Together, these constraints motivate a dedicated automated solution that ensures consistent, accurate, and reliable embedding of brass inserts. Technically, such a system must address several unmet needs: precise registration between CAD-defined coordinates and the physical part; closed-loop control of insertion depth and temperature to keep the polymer within a safe viscosity window; stable, low-runout mechanics to avoid lateral shear during seating; and robust singulation/feeding to eliminate jams and double-picks.

3. SYSTEM DESIGN

3.1. XY Motion System

The developed system is centered on a mechanically robust and modular architecture designed to ensure accurate positioning and repeatable insertion of brass threaded inserts.

The motion assembly employs an H-structure configuration for the tool head, providing a rigid and compact frame for XY displacement. Movement across the XY plane is achieved through a single continuous belt driven by two stepper motors, enabling synchronized and precise positioning over the entire work area while reducing mechanical complexity compared to dual-belt systems, as presented in Fig. 1.

Fig. 1. Single belt XY motion system.

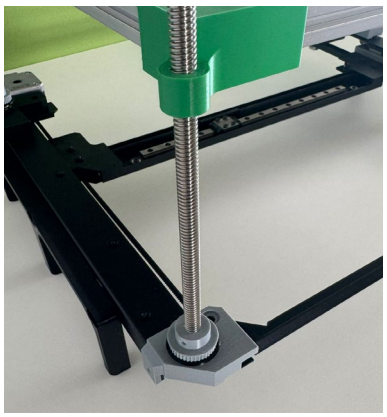

Fig. 2. Trapezoidal screw assembly for Z-axis motion.

3.2. Z-Axis Assembly

Vertical motion of the inverted bed is facilitated by four trapezoidal screws arranged at the corners of the structure. These screws are mechanically linked and driven in unison through a dedicated belt system, ensuring uniform lifting and lowering of the head along the Z-axis. This synchronized mechanism minimizes angular deviations and contributes to the overall stability of the insertion process, as presented in Fig. 2. This assembly is only used to set the "0" Z position for the tool, as the tool will have its own mechanism for inserting the brass inserts into the part.

3.3. Insertion Module

The insertion module itself is designed around a dual pinion with double helix rack-and-pinion assembly, where motion is transmitted symmetrically to maintain axial alignment, presented in Fig. 3. A spring element is integrated into the assembly to compensate for insertion force variations and to reduce the risk of damaging the printed part during embedding. Heating of the brass inserts is carried out using a standard soldering iron with an insertion heating tool, end mounted directly on the effector, ensuring sufficient thermal energy for reliable bonding between the insert and the polymer matrix.

3.4. Depth Control System

A key innovation is the integration of a capacitive touch sensor into the tool head, which detects when the insert reaches the proper depth by sensing contact with the workpiece surface. The sensor provides real-time feedback to the control software, halting the insertion module upon achieving the target depth, preventing over-penetration or under-insertion. This enhances repeatability and adapts to material variations (e.g., thermal expansion differences between PLA and ABS),

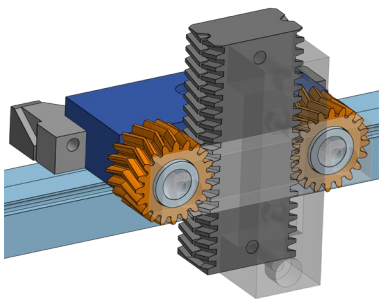

Fig. 3. Insertion module, part of the end effector.

Fig. 4. Workpiece fixture assembly.

addressing a critical need for precise depth control in automated insert placement.

3.5. Workpiece Fixture

Unlike conventional systems, like 3D printers, where the part is fixed below the tool, the printed component in this system is held above the tool head in a fixture, as presented in Fig. 4. This inverted bed configuration, which allows easier access for insert placement and minimizes the risk of part displacement during insertion. The fixture ensures stable clamping of the workpiece held in the insertion tool by gravity and provides compatibility with a range of part geometries.

Overall, the combination of a simplified belt-driven XY motion system, synchronized Z-axis actuation, thermally assisted insertion, and a dedicated clamping mechanism results in a system capable of performing accurate, repeatable, and fully automated brass inserts placement in 3D printed parts.

4. SOFTWARE IMPLEMENTATION

4.1. System Calibration

To ensure precise alignment, the system conducts a first-time calibration using the tool head's capacitive touch sensor to determine the real position of the work bed relative to the tool head.

The sensor detects contact with the bed surface, verifying the physical (0, 0) XY origin and adjusting the coordinate system to account for any positional discrepancies, ensuring accurate translation between virtual and physical spaces.

4.2. CAD Data Retrieval

The control software orchestrates the system's operation through a series of interconnected scripts implemented in Python, interfacing with the Onshape API [6] and the motion controller.

An initial script retrieves all mate connectors from the specified Onshape document via its URL, extracting and storing the coordinates of each connector, as shown in Fig. 5.

Mate connectors are strategically placed in the CAD model: one designated as "Base" serves as the reference point, corresponding to the (0, 0) XY origin on the physical work plate. All other mate connectors are defined relative to this base, accounting for the physical mounting orientation of the workpiece to ensure accurate translation between virtual and physical spaces.

```
data = json.loads(response.data)

# Transformarea la nivel de occurrence
occ = data["rootAssembly"]["occurrences"][0]["transform"]
T_occ = self._matrix_from_flat(occ)

origins_mm = {}
for feature in data["rootAssembly"]["features"]:
    if feature.get("featureType") != "mateConnector":
        continue
    name = feature["featureData"].get("name", feature.get("name", "<unnamed>"))
    mc = feature["featureData"]["mateConnectorCS"]
    R = np.array([mc["xAxis"], mc["yAxis"], mc["zAxis"]]).T   # 3×3
    t = np.array(mc["origin"])                                # 3
    T_mc = np.eye(4); T_mc[:3,:3] = R; T_mc[:3,3] = t

    T_abs = T_occ.dot(T_mc)
    # extrag metrii si convertesc in mm
    pos_m = T_abs[:3, 3]
    if round_coordinates:
        origins_mm[name] = np.round((pos_m * 1000.0), 2)
    else:
        origins_mm[name] = pos_m * 1000.0

return origins_mm
```

Fig. 5. Coordinate fetching from Onshape.

4.3. Coordinate Transformation

Upon fetching the coordinates, the software computes relative positions by subtracting the base coordinates from each insert location, generating a sequence of target points. These are then translated into motion commands for the XY gantry and Z-axis drive, as described in Fig. 6. The machine sequentially navigates to each computed point, positioning the tool head for embedding, using the code present in Fig. 7 to drive the stepper motors.

4.4. Embedding Process

During the embedding process, the tool head's tip collects a single brass threaded insert from the feeding mechanism. The insert is then heated to a material-specific temperature to facilitate secure bonding without compromising part integrity. Recommended temperatures, derived from established practices in additive manufacturing, are as follows: 225°C for PLA, 265°C for ABS, 260°C for ASA, 200°C for TPU, and 245°C for PETG [7].

These values ensure sufficient melting of the thermoplastic matrix for insert retention while minimizing thermal degradation. A thermocouple provides closed-loop feedback for precise temperature regulation.

4.5. Automated Insert Feeding

Post-embedding, the tool head retracts and moves to a predefined collection station to acquire the next insert

```
origins = self.fetch_mate_coords(round_coordinates=False)

if reference_mate not in origins:
    raise KeyError(f"Mate de referință '{reference_mate}' nu există")
# 2) Build inverse transform of reference in meters:
ref_mm = origins[reference_mate]
ref_m  = ref_mm / 1000.0
T_ref = np.eye(4); T_ref[:3,3] = ref_m
T_ref_inv = self._invert_transform(T_ref)

relative_mm = {}
for name, pos_mm in origins.items():
    # 3) go to meters, apply inverse, back to mm
    p_m     = pos_mm / 1000.0
    p4      = np.hstack([p_m, 1.0])
    p_rel_m = T_ref_inv.dot(p4)[:3]
    rel_mm  = p_rel_m * 1000.0

    # 4) round each component to 2 decimals if requested
    rel_mm = np.round(rel_mm, 2)
    relative_mm[name] = rel_mm

return relative_mm
```

Fig. 6. Transformation of absolute coordinates in relative coordinates to the “Base” mate connector.

```
for mate in mates:
    try:
        relatives = onshape.relative_distance_from_ref(mate)
        norm_relatives = onshape.to_pure_floats(relatives)
        next_mate = norm_relatives[mates[index]]
        print(f'Next mate is:{mates[index]} at {next_mate}')
        goto_x = next_mate[0]
        goto_y = next_mate[1]
        next_pose = [goto_x, goto_y]
        axis_system.go_to_relative(next_pose)
        last_pose = axis_system.position
```

Fig. 7. Navigation routine of the end effector.

from the vibratory bowl feeder via the linear track, enabling continuous operation across multiple placement sites.

5. TESTING PHASE

The testing campaign quantified XY positional accuracy, Z insertion depth, and cycle time per insert, while validating short-term repeatability and tool thermal stability. We also benchmarked the automated process against manual heat-set insertion to measure efficiency and variability gains and to identify dominant failure modes – misfeeds, tilt, cold welds, and boss deformation – with their causes. Test articles were PLA and ABS coupons and bosses printed from single-lot filaments; geometries used guide holes for M3/M4 and top-down access. Perimeters were set to 3, 4, 5 and 6, (including both internal and external perimeters), printed in both orientations normal (Fig. 8) and parallel to the bed – (Fig. 9), printed at 0.2 mm layer heights, using a standard 0.4 mm nozzle. Brass M3/M4 inserts from one lot were used, with ≥ 30 insertions per condition for statistical confidence.

Instrumentation prioritized traceable metrology. XY homed on optical end-stops; Z zeroed on a hard stop then fine-calibrated via the capacitive sensor on a gauge block. XY error was measured by a vision system (5–10 µm pixel scale) or CMM; depth by dial indicator/contact probe referenced to the surface. A tool-tip thermocouple was logged at 1 Hz at 225 °C (PLA) and 265 °C (ABS). Controller timestamps segmented approach, dwell, press,

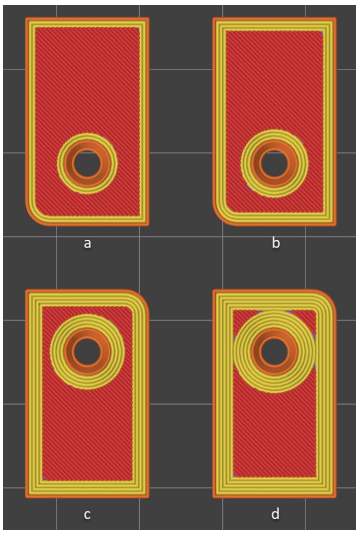

Fig. 8 Parts printed with holes normal to the bed: *a* – 3 perimeters; *b* – 4 perimeters; *c* – 5 perimeters; *d* – 6 perimeters.

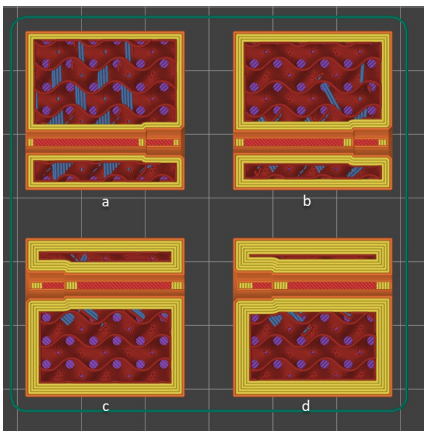

Fig. 9. Parts printed with holes parallel to the bed: *a* – 3 perimeters; *b* – 4 perimeters; *c* – 5 perimeters; *d* – 6 perimeters

and retract. A Gage R&R (Gage Repeatability & Reproducibility – GRR) (10 parts × 3 repeats × 2 appraisers) kept measurement variation under 10% of total.

Experiments used fixed baselines for approach speed, press profile, dwell, temperature, and feeder timing, plus a screening design varying the total perimeters (3 to 6), hole tolerance (−0.05/0/+0.05 mm), approach speed (slow/nominal/fast), dwell (−20%/nominal/+20%), and temperature (−10/nominal/+10 °C). Responses were XY radial error, depth error versus 6 mm (M3) and 8 mm (M4), cycle time, and boss flatness. Each run began after tip stabilization within ±2–3 °C for ≥2 min. Parts were clamped in the inverted vise, Z0 probed, and CAD coordinates imported and validated on two fiducials. A manual benchmark used an experienced operator with the same brand and model of temperature-controlled iron under identical metrology.

Data processing computed radial XY error from axis residuals and reported mean, standard deviation (SD), and 95% confidence intervals; depth accuracy was the signed error to target. Repeatability used short-term SD and capability indices C_p and C_{pk} against ±0.10 mm limits in XY and Z. Acceptance criteria required mean XY ≤ 0.07 mm with SD ≤ 0.04 mm, mean depth within ±0.05 mm with SD ≤ 0.04 mm, thermal ripple ≤ ±3 °C, ≤ 2% defects over 100 cycles, and ≥ 20% throughput gain versus manual.

Observed failures were rare: misfeeds traced to stacked/ovalized inserts were eliminated with an anti-stack escapement and chamfered rails; tilt from warped surfaces was reduced by fitting a local plane from three probes; ABS cold welds disappeared with +15% dwell or +5 °C; incipient boss collapse was prevented by limiting press velocity and enforcing a force threshold with immediate retract. Current tests covered flat coupons and simple bosses in lab conditions; future work will address curved/recessed surfaces, multi-level fixtures, environmental sweeps, and torque-out/pull-out testing to link metrology to joint strength.

6. RESULTS AND DISCUSSIONS

The automated system demonstrated superior performance across all tested conditions, leveraging the precision of MOONS MS17HD2P4100 stepper motors and DRV8825 drivers with microstepping capabilities. The software consistently sequenced M3 and M4 inserts correctly, as defined by the Onshape mate connectors, with no errors in insertion order observed. Tables 1–3 summarize the results.

The results confirm the system's high precision, with positional accuracy ranging from ±0.05 mm to ±0.07 mm, surpassing the industry standard of ±0.10 mm for threaded joints. PLA samples exhibited slightly better accuracy due to lower thermal expansion compared to ABS. Embedding times were faster for PLA (3.8–4.2 s) than ABS (4.2–4.6 s) due to lower melting temperatures, with minimal impact from number of perimeters. M4 inserts required slightly longer embedding times due to larger holesizes. Repeatability remained high, with standard deviations of 0.025–0.035 mm, attributed to the

Table 1

Positional Accuracy by Material, Perimeters and Insert Size

Material	Perimeters	Insert Size	Manual Accuracy (mm)	Automated Accuracy (mm)	Improvement (%)
PLA	3	M3	±0.25	±0.05	80
PLA	3	M4	±0.25	±0.05	80
PLA	4	M3	±0.24	±0.05	79
PLA	4	M4	±0.24	±0.05	79
PLA	5	M3	±0.24	±0.06	75
PLA	6	M4	±0.24	±0.06	75
ABS	3	M3	±0.26	±0.06	77
ABS	3	M4	±0.26	±0.06	77
ABS	4	M3	±0.25	±0.06	76
ABS	4	M4	±0.25	±0.06	76
ABS	5	M3	±0.25	±0.07	72
ABS	6	M4	±0.25	±0.07	72

Table 2

Embedding Time by Material, Perimeters and Insert Size

Material	Perimeters	Insert Size	Manual Time (s)	Automated Time (s)	Improvement (%)
PLA	3	M3	15.0	3.8	75
PLA	3	M4	15.5	4.0	74
PLA	4	M3	15.2	3.9	74
PLA	4	M4	15.7	4.1	74
PLA	5	M3	15.4	4.0	74
PLA	6	M4	15.9	4.2	74
ABS	3	M3	16.0	4.2	74
ABS	3	M4	16.5	4.4	73
ABS	4	M3	16.2	4.3	73
ABS	4	M4	16.7	4.5	73
ABS	5	M3	16.4	4.4	73
ABS	6	M4	16.9	4.6	73

Table 3

Placement Depth Repeatability

Material	Perimeters	Insert Size	Automated Standard Deviation (mm)
PLA	3	M3	0.025
PLA	3	M4	0.026
PLA	4	M3	0.027
PLA	4	M4	0.028
PLA	5	M3	0.030
PLA	6	M4	0.031
ABS	3	M3	0.030
ABS	3	M4	0.031
ABS	4	M3	0.032
ABS	4	M4	0.033
ABS	5	M3	0.034
ABS	6	M4	0.035

precision of the MOONS stepper motors and microstepping drivers. Compared to Hanga et al. [2–3], the system offers simpler integration with additive manufacturing workflows due to its Onshape compatibility and automated feeding. Potential errors, such as feeder jams or thermal variations, were mitigated through calibration but warrant further study.

7. FUTURE WORK

Future work targets an adaptive tool head for complex geometries (curved surfaces, multi-axis orientations), implemented via a 5-axis stage or interchangeable end-effectors for flexibility. The feeding system will add smart sorting that auto-detects, and sequences insert sizes/types without user preloading. Motion planning will be upgraded with S-curve profiles to cut vibration, boost speed, and reduce mechanical wear. We will extend compatibility to larger sizes (e.g., M6) and new materials (polycarbonate, nylon) and integrate machine vision for real-time defect detection plus AI-based control that tunes embedding parameters on the fly. Finally, we'll assess scalability to high-volume lines and generalize the platform to related post-processes such as press-fitting, riveting, and other AM finishing steps.

8. CONCLUSIONS

This study presents a fully CAD-guided automated system for embedding brass threaded inserts into 3D-printed parts and shows clear gains in precision (±0.05–0.07 mm), efficiency (73–75% faster than manual insertion), and repeatability (0.025–0.035 mm standard deviation). By reading insert coordinates directly from Onshape and executing them on a robust motion platform driven by MOONS stepper motors, the approach closes the loop between digital design intent and physical assembly. Closed-loop depth control via a capacitive touch sensor establishes the workpiece reference and

verifies target seating depth (e.g., 6 mm for M3, 8 mm for M4), while thermocouple feedback at material-appropriate setpoints (≈ 225 °C for PLA and ≈ 265 °C for ABS) maintains a stable thermal window during insertion. The gravity-tube storage and servo-actuated escapement singulate inserts reliably, reducing operator dependence and minimizing misfeeds without compromising throughput. Across PLA, ABS, PETG, and varied perimeters, the system holds tight positional and depth tolerances, demonstrating robustness uncommon in manual heat-set methods. Beyond raw performance, it delivers a traceable, data-rich workflow: temperatures, depth triggers, and cycle timestamps are logged for statistical process control.

The current results validate the concept at the work-cell level and outline a clear path to scale. Near term, we will add an adaptive tool head for recessed/curved surfaces, smarter feeding with jam-tolerant geometry and sensorized state detection to remove manual sequencing, and motion-planning refinements that smooth approach/press profiles to limit boss deformation. Finally, broader validation, torque-out/pull-out across materials and geometries, environmental robustness (humidity/temperature sweeps), and multi-shift endurance, that will complete the evidence base for industrial adoption and enable fully automated, in-line post-processing in additive manufacturing lines.

REFERENCES

[1] Nefelov, I.S.; Baurova, N.I. *Formation of Threaded Surfaces in the Components Produced by 3D Printing*. Russ. Metall. (Metally) 2017, 2017, 1158-1160. DOI:10.1134/S0036029517130183.

[2] Kastner, T.; Troschitz, J.; Vogel, C.; Behnisch, T.; Gude, M.; Modler, N. *Investigation of the Pull-Out Behaviour of Metal Threaded Inserts in Thermoplastic Fused-Layer Modelling (FLM)* Components. J. Manuf. Mater. Process. 2023, 7(1), 42. DOI:10.3390/jmmp7010042.

[3] Hanga, M.; Drăguțu, M.; Nașu, T.-C.; Cazacu, C.-C.; *Automatic CNC System for metal inserts in 3D printed parts*, Journal of Industrial Engineering and Robotics, accepted/in press.

[4] Zi, B.; Wang, N.; Qian, S.; Bao, K.; *Design, stiffness analysis and experimental study of a cable-driven parallel 3D printer*. Mech. Mach. Theory 2019, 132, 207-222. DOI:10.1016/j.mechmachtheory.2018.11.003.

[5] Tu, J.-C.; Wang, Y.-L.; Wang, J.-C.; Ksica, F.; Hadas, Z. *Development of Integrated 3D Printing and Automated Embedding System*. IEEE Proceedings 2024. DOI:10.1109/ME61309.2024.10789740.

[6] *Introduction to the Onshape REST API,* available at: `https://onshape-public.github.io/docs/api-intro/`, accessed: 20.07.2025.

[7] S. Hermans, *Tips & Tricks for Heat-Set Inserts used in 3D printing,* available at: `https://www.cnckitchen.com/blog/tipps-amp-tricks-fr-gewindeeinstze-im-3d-druck-3awe`, accessed: 20.07.2025.